

Supporting Information

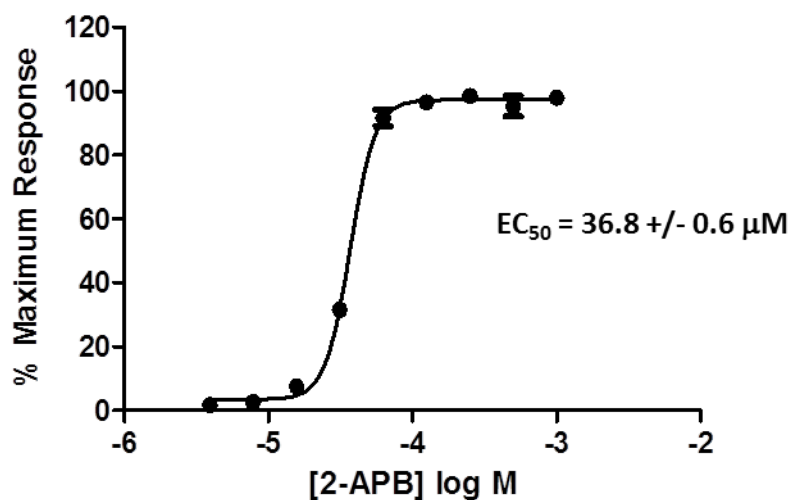
Synthesis and Pharmacology of (Pyridin-2-yl)methanol Derivatives as Novel and Selective Transient Receptor Potential Vanilloid 3 Antagonists

Arthur Gomtsyan,* Robert G. Schmidt, Erol K. Bayburt, Gregory A. Gfesser, Eric A. Voight, Jerome F. Daanen, Diana L. Schmidt, Marlon D. Cowart, Huaqing Liu, Robert J. Altenbach, Michael E. Kort, Bruce Clapham, Phil B. Cox, Anurupa Shrestha, Rodger Henry, David N. Whittern, Regina M. Reilly, Pamela S. Puttfarcken, Jill-Desiree Brederson, Ping Song, Bin Li, Susan M. Huang, Heath A. McDonald, Torben R. Neelands, Steve P. McGaraughty, Donna M. Gauvin, Shailen K. Joshi, Patricia N. Banfor, Jason A. Segreti, Mohamad Shebley, Connie R. Faltynek, Michael J. Dart, Philip R. Kym

Research & Development, AbbVie Inc., 1 North Waukegan Road, North Chicago, Illinois 60064, United States

Table of Contents

2-APB concentration-response curve	S2
Cerep selectivity data for 74a	S2
Kinome selectivity data for 74a	S3
Bioprofiling selectivity data for 74a	S4
Rat cardiovascular safety profile of 74a	S5
Relative stereochemistry determination of 7 , 8 , 60f , 61f , 62f and 63f by 2D-NMR	S6
Electrophysiology method description	S7
In vivo efficacy (SNL, CC and reserpine model)	S8
X-ray crystallographic data	S10
References	S11



Supplemental Figure 1. 2-APB concentration-response curve in HEK293/human TRPV3 cells. Influx of Ca²⁺ into recombinant HEK293/human TRPV3 cells activated by 2-APB as monitored by FLIPR. Data represent the mean +/- S.E.M. of three determinations.

Supplemental Table 1. Profile of **74a** in CEREP panel of receptor binding assays

Assay	Percent Inhibition	Assay	Percent Inhibition
5-HT transporter	-9	ETB	-6
5-HT1A	4	GABA	9
5-HT1B	-12	GAL1	-17
5-HT2A	5	GAL2	-18
5-HT2B	-16	GR	-4
5-HT2C	-11	H1	-3
5-HT3	1	H2	-18
5-HT5a	-17	IP (PGI2)	-11
5-HT6	8	kappa (KOP)	11
5-HT7	13	KV	5
A1	-9	M1	-5
A2A	-1	M2	1
A3	-6	M3	0
alpha 1	-12	M4	6
alpha 2	-6	M5	8
AT2	-4	MAO-A	3

B2	-3	MC4	-8
BB	-10	MT1 (ML1A)	2
beta 1	-4	mu (MOP)	-1
beta 2	0	NK1	-17
BZD (central)	-28	NK2	-10
BZD (peripheral)	-7	NK3	7
Ca ²⁺ channel(L, verapamil site)	3	NOP (ORL1)	-2
CB1	15	norepinephrine transporter	0
CCK1 (CCKA)	-26	NTS1 (NT1)	-20
CCK2 (CCKB)	-24	P2X	-8
CCR1	-9	P2Y	7
CGRP	-12	PAC1 (PACAP)	-8
Cl channel	3	PCP	2
CXCR2 (IL-8B)	6	PDGF	-11
D1	1	PPARgamma	1
D2S	8	sigma	-2
D3	8	SKCa channel	-1
D4.4	3	sst (non-selective)	-8
D5	-13	TNF-alpha	-4
dopamine transporter	-6	VPAC1 (VIP1)	4
EP2	23	Y1	-10
ETA	4	Y2	-18

Supplemental Table 2. Profile of **74a** in AbbVie kinome panel assays

Assay	IC ₅₀ (μM)	Assay	IC ₅₀ (μM)
ACVR1	>10	MAP2K3	>10
ALK	>10	MAP3K10	>10
Abl	>10	MAP4K2	>10
Akt1	>10	MAP4K4	>10
Aurora1	>10	MEK1	>10
Aurora2	>10	MEK2	>10
BRAF	>10	MST1	>10
BTK	>10	Nek2	>10
CAMK1D	>10	PAK4KD	>10
CAMK2A	>10	PDGFRA V561D	>10
CAMKK2	>10	PDGFRB	>10
CDK11	>10	PKA	>10
CDK7/Cyclin H/Mat1	>10	PKCtheta	>10
CDK8/Cyclin C	>10	PKCzeta	>10
CDK9/Cyclin K	>10	PKG1A	>10
CLK2	>10	Pim1	>10
CSF1R	>10	Pim2	>10
Cklalpha1	>10	Plk3	>10

DDR1	>10	Prkc	>10
DYRK1B	>10	RET	>10
Dyrk1A	>10	Rock1	>10
EGFR	>10	Rock2	>10
Erk2	>10	Rsk2	>10
FAK	>10	SGK1	>10
FGFR1	>10	STK16	>10
Flt1	>10	STK33	>10
Fyn	>10	Src	>10
GRK5	>10	Syk CatDom	>10
Gsk3a	>10	TAOK2	>10
Gsk3b	>10	TBK1	>10
IGF1R	>10	TNK2	>10
IKKE	>10	TYRO3	>10
InsR	>10	TrkA	>10
JAK2	>10	TrkB	>10
JAK3	>10	TrkC	>10
JNK1	>10	Wee1	>10
JNK2	>10	Zipk	>10
Kdr	>10	cMET	>10
LTK	>10	cdk2	>10

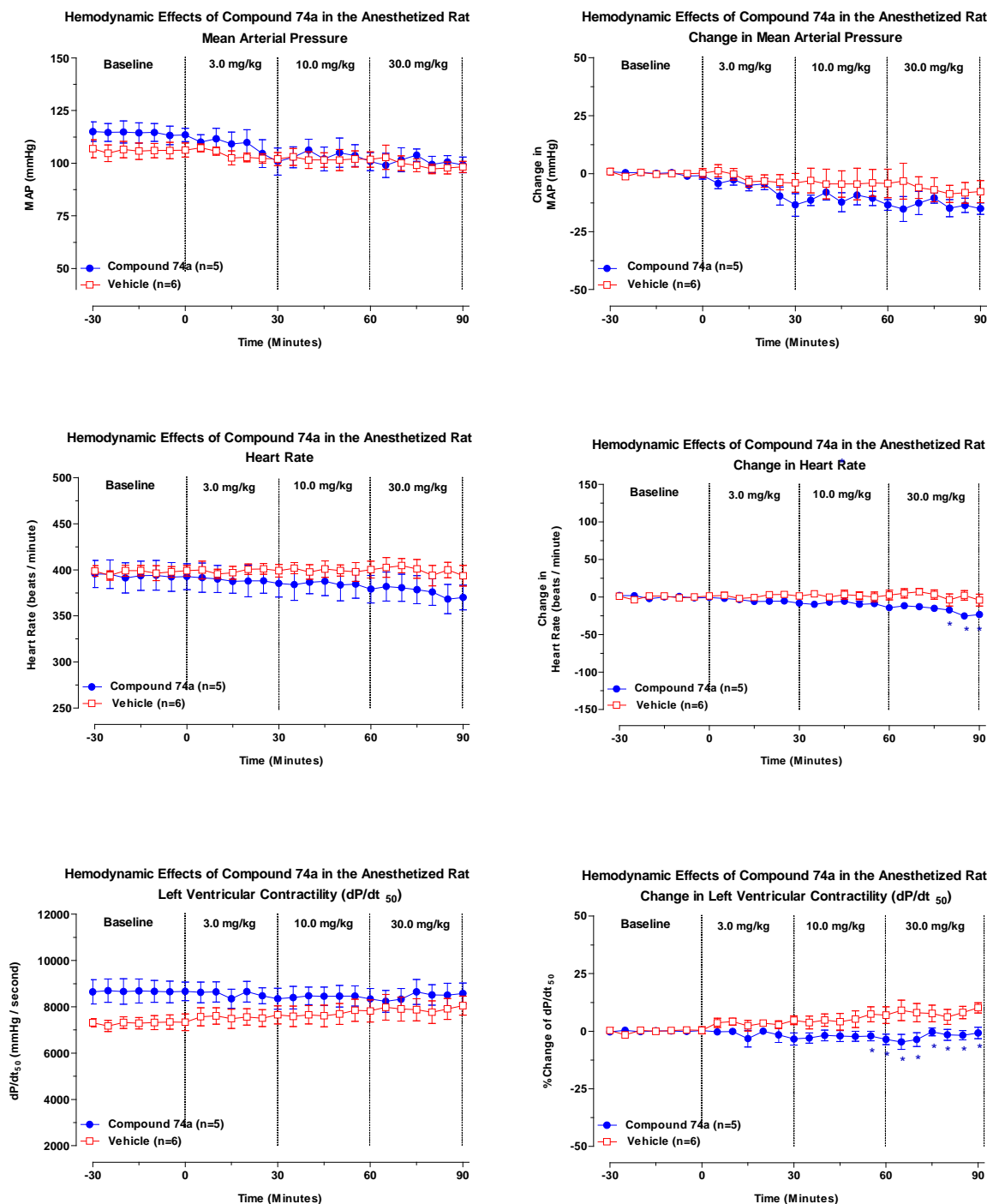
Supplemental Table 3. Profile of **74a** in AbbVie panel of receptor binding assays

Assays	EC ₅₀ (μM)	Assays	IC ₅₀ (μM)
5HT1A	>10	hERG	>30
5-HT2A	>10	PDE3A	>10
5-HT2B	>10	PDE4B2	>10
5-HT2C	>10	5-HT1A	>10
A1	>10	5-HT2A	>10
AT1	>10	5-HT2B	>10
Alpha1A	>10	5-HT2C	>10
Alpha2A	>10	A1	>10
B2	>10	AT1	>10
Beta1	>10	Alpha1A	>10
CB1	>10	Alpha2A	>10
Cav1.2 (L-type)	>10	B2	>10
D2L	>10	Beta1	>10
ETA	>10	CB1	>10
ETB	>10	Cav1.2 (L-type)	NV
H1	>10	D2L	>10
M2	>10	ETA	>10
Opioid mu	>10	ETB	>10

PPARgamma	>10	H1	>10
TRPV1	>37.5	M2	>10
Na _v 1.7	>20	Opioid mu	>10
TrkA	>50	P2Y	>10

Supplemental Figure 2. Rat cardiovascular safety of **74a**

Hemodynamic Effects of Compound 74a in the Anesthetized Rat



Supplemental Figure 3. Relative stereochemistry determination by 2D-NMR

A.



Compound **7** was characterized by ^1H , COSY, ROESY, and HSQC experiments. Data collected are consistent with the proposed stereochemistry. In the ROESY spectrum aryl proton "1" and methine proton "3" show a common NOE to methylene proton "2b". This suggests a *trans* - relationship between the two aryl rings in the molecule. Compound **8** was characterized by ^1H , COSY, ROESY, and HSQC experiments. Data collected are consistent with the proposed stereochemistry. In the ROESY spectrum aryl protons "1" and "4/5" show a common NOE to methylene proton "2a" while methine "3" shows a stronger NOE to methylene "2b". This suggests a *cis*- relationship between the two aryl rings in the molecule.

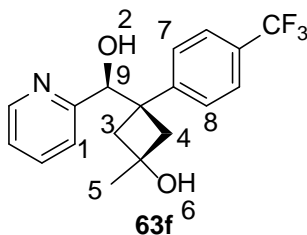
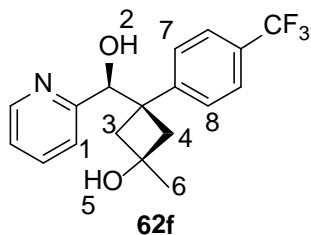
B



Compound **60f** was characterized by ^1H , COSY, ROESY, HSQC and HMBC experiments in DMSO- d_6 at room temperature. Chemical shift assignments were made based on the collected 2D data. Data collected are consistent with the shown stereochemistry. In the ROESY spectrum an NOE correlation was observed from methine "3" to aryl proton "1" and methine proton "2". Compound **61f** was characterized by ^1H , COSY, ROESY, HSQC and HMBC experiments in

DMSO-d₆ at room temperature. Chemical shift assignments were made based on the collected 2D data. Data collected are consistent with the shown stereochemistry. In the ROESY spectrum an NOE correlation was observed between methine "3" and aryl protons "4/5".

C.



H-H ROESY NMR data for **62f** support the methyl group on the cyclobutane and the benzene ring are *cis* relative to each other. Protons H3a and H4a have NOE correlations to both the methyl H6 protons and the benzene ring protons (H7 and H8). On the other face of the cyclobutyl ring, H3b and H4b have NOE to OH 5, pyridyl proton H1 and OH 2. H-H ROESY NMR data for **63f** support the conclusion that the benzene ring and the hydroxyl group on the cyclobutyl ring are in *cis* relationship to each other. In the H-H ROESY NMR studies, protons H3a/H4a (same face of cyclobutyl) have NOE correlations to the benzene protons (H7/H8) and the hydroxyl proton H6. On the other face of the cyclobutyl ring, H3b/H4b have NOE to methyl H5 and methine H9 and pyridyl H1.

Electrophysiology. Electrophysiological evaluation of TRPV3 antagonist **74a** was performed according to the methodology previously described for TRPV1¹ with the following exceptions. Stock of the agonist, 2APB (Tocris) was made at 100 mM in DMSO and stored in the freezer. On the day of the experiment, the stock was diluted 1:1000 in external buffer. TRPV3 currents were recorded by a 160 ms ramp protocol (-80 to +80 mV) every second. Current amplitudes in response to agonist and antagonists were measured at both -80 and

+80 mV.

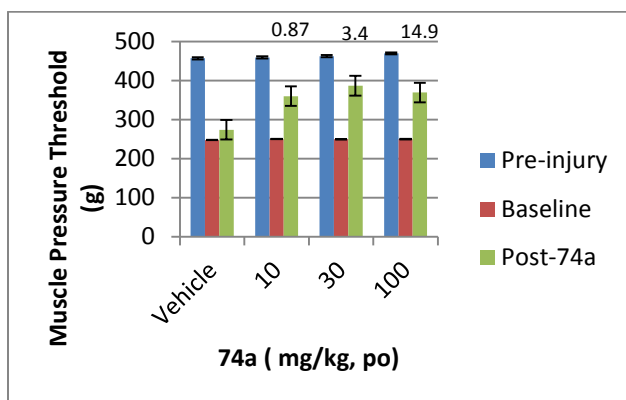
In Vivo Evaluation. Male Sprague-Dawley rats (neuropathic models, Charles River, Wilmington, MA; reserpine model, Harlan, Indianapolis, IN) weighing 200–300 g were utilized. All animals were group housed in AAALAC approved facilities at AbbVie in a temperature-regulated environment with lights on between 0700 and 2000 h. Food and water were available ad libitum except during testing. All animal handling and experimental protocols were approved by an Institutional Animal Care and Use Committee (IACUC). All experiments were performed during the light cycle. Unless otherwise noted, all experimental and control groups contained at least six animals per group and data are expressed as mean (\pm SEM). Data analysis was conducted using analysis of variance and appropriate posthoc comparisons ($P < 0.05$) as previously described.²

Spinal Nerve (L5/L6) Ligation Model of Neuropathic Pain. As previously described in detail, a 1.5 cm incision was made dorsal to the lumbosacral plexus in anesthetized rats.³ The paraspinal muscles (left side) were separated from the spinous processes, and the L5 and L6 spinal nerves were isolated and tightly ligated with 3-0 silk threads. Following hemostasis, the wound was sutured and coated with antibiotic ointment. The rats were allowed to recover and then placed in a cage with soft bedding for 14 days before behavioral testing for mechanical allodynia.

Chronic Constriction Injury Model of Neuropathic Pain. As previously described in detail, a 1.5 cm incision was made 0.5 cm below the pelvis in anesthetized rats.⁴ The biceps femoris and the gluteous superficialis (right side) then were separated. The sciatic nerve was exposed, isolated, and four loose ligatures (5-0 chromic catgut) with 1 mm spacing were placed around it. The rats were allowed to recover and then placed in a cage with soft bedding for 14 days prior to behavioral testing for mechanical allodynia. Animals were tested for mechanical allodynia using

calibrated von Frey filaments (Stoelting, Wood Dale, IL). Briefly, rats were placed into individual Plexiglas containers and allowed to acclimate for 15-20 min before testing. Paw withdrawal threshold was determined by increasing and decreasing stimulus intensity and estimated using a Dixon nonparametric test. Only rats with threshold scores of 4.5 g were considered allodynic and utilized in compound testing experiments.

Reserpine model of central pain. As previously described in detail rats received a subcutaneous injection of reserpine (1 mg/kg) daily for 3 days in alternating injection sites.^{5,6} Mechanical hyperalgesia was assessed 4 days following the last reserpine injection using a Randall Siletto paw pressure device placed over the mid-gastrocnemius muscle until a nocifensive behavior (withdrawal, struggling, or vocalization) was observed. One reading was taken at each time point (pre-injury, baseline, 1, 2, or 4 h; 2 and 4 h time point data not shown), with a maximum stimulus intensity of 500 g. Plasma was collected after the last dose and assessed for concentration of **74a**.



Supplemental Figure 3. Compound **74a** (10, 30, 100 mg/kg po) was anti-nociceptive in the reserpine model of central pain. The compound dose-dependently increased muscle pressure threshold induced by reserpine at 1 h post dosing ($P < 0.05$ Dunnett's post hoc test versus vehicle). Plasma levels for **74a** are shown above the compound treated group bars.

X-Ray Crystallographic Analysis of **5a**, **5a** as HCl salt, (*R*)-**5h**, **15** and **37a**



Compound (R)-5hIHCL.cif



Compound 5a.cif



Compound 5aHCL.cif



Compound 15.cif



Compound 37a.cif

References

1. Neelands, T. R.; Jarvis, M. F.; Han, P.; Faltynek, C.R.; Surowy, C. S.; Acidification of rat TRPV1 alters the kinetics of capsaicin responses. *Mol. Pain* **2005**, *1*, 28.
2. Joshi, S. K.; Hernandez, G.; Mikusa, J. P.; Zhu, C. Z.; Zhong, C.; Salyers, A.; Wismer, C. T.; Chandran, P.; Decker, M. W.; Honore, P. Comparison of antinociceptive actions of standard analgesics in attenuating capsaicin and nerve-injury-induced mechanical hypersensitivity. *Neuroscience* **2006**, *143*, 587–596.
3. Kim, S. H.; Chung, J. M. An experimental model for peripheral neuropathy produced by segmental spinal nerve ligation in the rat. *Pain* **1992**, *50*, 355–363.
4. Bennett, G. J.; Xie, Y. K. A peripheral mononeuropathy in rat that produces disorders of pain sensation like those seen in man. *Pain* **1988**, *33*, 87–107.
5. Nagakura, Y.; Oe, T.; Aoki, T.; Matsuoka, N. (2009) Biogenic amine depletion causes chronic muscular pain and tactile allodynia accompanied by depression: A putative animal model of fibromyalgia. *Pain* **2009**, *146*, 26-33.
6. Nagakura, Y.; Takahashi, M.; Noto, T.; Sekizawa, T.; Oe, T.; Yoshimi, E.; Tamaki, K.; Shimizu, Y. Different pathophysiology underlying animal models of fibromyalgia and neuropathic pain: Comparison of reserpine-induced myalgia and chronic constriction injury rats. *Behav. Brain Res.* **2012**, *226*, 242-249.

